

# Optical properties of Rydberg excitons in Cu<sub>2</sub>O based superlattices

David Ziemkiewicz,\* Gerard Czajkowski, and Sylwia Zielińska-Raczyńska  
*Institute of Mathematics and Physics, UTP University of Science and Technology,  
Al. Prof. S. Kaliskiego 7, 85-789 Bydgoszcz, Poland*  
(Dated: February 19, 2025)

Combining the microscopic calculation of superlattice minibands and the macroscopic real density matrix approach one can obtain electric susceptibilities of the superlattice system irradiated by an electromagnetic wave. It is shown how to compute the dispersion relation, excitonic resonances positions and susceptibility of Cu<sub>2</sub>O/MgO based superlattice (SL), when Rydberg Exciton-Polaritons appear, including the effect of the coherence between the electron-hole pair and the electromagnetic field and the polaritonic effect. Using the Kronig-Penney model for computing miniband SL parameters the analytical expressions for optical functions are obtained and the numerical calculations for Cu<sub>2</sub>O/MgO SL are performed.

PACS numbers: 78.20.ae, 71.35.Cc, 71.36.+c

## I. INTRODUCTION

Excitons, Coulomb-bound pairs of a one conduction band electron and a one valence band hole, form an electrical neutral quasiparticle, transferring the energy without transporting the net electric charge<sup>1</sup>. These quasiparticles are complex many-body states embedded in the background of crystal lattice, which interact via scattering, phase-space and screening. Therefore the problem of a manipulation of exciton states through application of artificial periodic potentials systems has attracted lot of attention; some implementations include colloidal semiconductor nanocrystals<sup>2</sup>, microrod arrays<sup>3</sup> and micropillars<sup>4</sup>. As pointed out in<sup>5</sup>, so-called structured excitons can be used as a means of transporting information and energy in quantum information processing. One of the ways to control these excitons is via superlattice<sup>6</sup>. Such a system causes a large shift of exciton energy states and thus influences optical and electronic properties. In principle, SL containing Rydberg exciton is a solid-state analogue of Rydberg atom trapped in an optical lattice, which are a promising tool in quantum computing<sup>7-9</sup>. Superlattice can also be used as a medium for exciton-exciton interaction experiments<sup>5</sup>. Importantly, superlattice has an advantage of relative simplicity and ease of fabrication. Moreover, in the case of Cu<sub>2</sub>O/MgO system proposed here, when low principal number excitons are used, room temperature operation is feasible<sup>10</sup>.

A superlattice is a periodic structure of layers made of two (or more) semiconductor or insulator materials with different band gaps, each quantum well sets up new selection rules that affect the conditions for charges to flow through the structure. The two different semiconductor materials are deposited alternately on each other to form a periodic structure in the growth direction. Typically the width of layers is order of magnitude larger than the lattice constant, and is limited by the growth of the structure. Due to the small width of individual layers, on the scale of illuminating light wavelength they merge together to form a homogeneous system, which behaves

like a bulk crystal. Important requirements of producing a superlattice are a small lattice mismatch and different band gaps energies between two material components of the structure.

Recently Yang *et al.*<sup>6</sup> produced SL based on cuprite, where the wells consist of a narrow-bandgap semiconductor Cu<sub>2</sub>O and the barriers are made of a wide-bandgap insulator MgO. The lattice constants of both these substances are quite similar with a small mismatch between the constituent layers (with the difference 1.35 %), while Cu<sub>2</sub>O is a narrow-band gap semiconductor with  $E_g \sim 2.2$  eV and MgO is a wide-band gap compound with  $E_g \sim 8$  eV<sup>6</sup>, which satisfy the basic requirements for a good SL structure.

In this paper, we consider a structure of similar dimensions, e.g. total thickness on the order of 100 nm and individual layer thickness on the order of few nm. We intend to describe optical properties of this SL: the optically active layers of cuprous oxide Cu<sub>2</sub>O and buffer layer of magnesium oxide MgO. In our paper we will discuss the behavior of Rydberg excitons located in the system of quantum wells, which create a system of periodic potentials. Since the first observation of Rydberg excitons (REs) in Cu<sub>2</sub>O in 2014<sup>11</sup>, they become a subject of intensive studies. These highly excited states in Cu<sub>2</sub>O, were observed up to a large principal quantum number  $n = 30$ <sup>12</sup>. Due to unusual properties of REs, such as huge sizes scaling as  $n^2$ , long life times reaching nano seconds, strong exciton-exciton interactions controlled by so-called Rydberg blockade, REs could have many promising applications as single-photon emitters, single photon transistors and as active medium of masers.<sup>13</sup> Initial studies on Rydberg excitons were focused at the optical properties of REs in high quality nature crystals (bulk crystals), see<sup>14,15</sup> for recent references. Also some groups concentrated on fabrication techniques of Cu<sub>2</sub>O nanostructures<sup>16,17</sup>. Recently, the main interest of research has shifted from REs in bulk crystals to excitons in low-dimensional systems<sup>18-20</sup>. The first experimental verification of an oscillator strength change caused by the quantum confinement of REs in low dimensional

quantum system<sup>21</sup> was an important step forward to exploit them in quantum applications. Therefore it seems natural to examine the optical properties of REs in the specific type of a nanosystem, which consists of quantum wells forming lattice of periodic potentials confining REs. The unique property of periodic potential systems is a possibility of changing effective masses of particles inside such structures. Regarding an exciton in SL, an electron and a hole effective masses are modified, which results in adjustment of an optical susceptibility. For a given SL structure geometry one is able to predict the shift of excitonic resonances positions comparing to the bulk case. The last but not the least argument for choosing this subject is the fact that the optical lattices with neutral atoms have been successfully applied in quantum information devices. In analogy we imply that due to the inherent, repeating pattern of and long-coherence times of Rydberg excitons, their huge polarizability and dipole moments, which allow them strongly interact with each other over a long distance, arranged in such systems, they might be also viable candidates for quantum computing.

Band-edge optical properties of superlattices can be discussed by modelling the superlattice as an effective anisotropic medium in which the quasi-free carriers propagate and interact. In the low barriers limit the electron and hole motion in the confinement direction is determined by the superlattice potential and is replaced by an effective-mass motion, with the appropriate effective masses obtained from the miniband dispersion relations<sup>22,23</sup>.

Since excitons in the majority of semiconductors are of Wannier type, the transition dipole has a spatial extension, characterizing the interaction of radiation with electrons and holes located at different sites. This results in a coherence between the electron-hole pair and the radiation field. In analogy to bulk semiconductor excitons, SL excitons induced by an electromagnetic wave propagating through the SL will give rise to “*SL-polaritons*”.

As in the bulk crystals, polaritons are mixed modes of the electromagnetic field and discrete excitations of the SL  $E_n(\mathbf{k}_{\text{ex}})$  (excitons). Below the gap one can imagine a polariton as a photon surrounded by a cloud of virtual electron-hole pairs (excitons).

All the above mentioned components (Wannier excitons, effective mass approximation, exciton-polaritons with coherence) justify the use of the Real Density Matrix Approach (RDMA) to describe optical properties of superlattices. The method has been already used to describe excitons and polaritons in III-V<sup>24</sup> and II-VI SL<sup>25</sup> and was successful in description of REs optical properties of Cu<sub>2</sub>O bulk crystals<sup>26</sup>, and nanostructures (quantum wells, dots and wires)<sup>27</sup>.

Below we present in details a procedure of calculation, which starts with the Kronig-Penney model to obtain SL miniband parameters i.e., anisotropic effective masses and band gaps. To derive the dispersion relation and resonance positions in SL, RDMA with these parameters is used. This method has general character, allows to get

analytical formula for a system susceptibility. It takes into account both the Coulomb interaction between an electron and a hole and coherence between an electron-hole pair and a radiation field. The particular calculations will be done for Cu<sub>2</sub>O/MgO SL, for which the SL dielectric tensor and the optical functions in the analytical form will be calculated.

The paper is organized as follows. In Sec. II we present the basic equations of the Kronig-Penney model adapted to the cases of superlattices. Sec. III shows the scheme for calculating SL optical functions in the case when the total thickness of the SL is much greater than the excitonic Bohr radius. In Sec. IV results obtained for Cu<sub>2</sub>O/MgO superlattice are discussed and conclusions are presented in Sec V.

## II. KRONIG-PENNEY MODEL FOR SUPERLATTICES

In this section we recall the basic equations which describe the electronic states (conduction and valence bands) of a superlattice. Considering the Kronig-Penney model we assume the confinement potential in the  $z$ -direction (structure growth direction), which for conduction electrons corresponds to  $V(z) = 0$  if  $z$  corresponds to area inside well, (well thickness  $L_W$ , effective mass  $m_W$ ), and  $V(z) = V_0$  if  $z$  corresponds to the barrier area (thickness  $L_B$ , effective mass  $m_B$ ), where  $V_B$  is the conduction band offset. The equation for the values of the Bloch vector  $K$ , and thus the miniband dispersion<sup>22–28</sup>, takes the Kronig-Penney form

$$\begin{aligned} \cos KL &= \cos k_1 L_W \cosh \kappa_2 L_B \\ &- \frac{k_1^2 - \kappa_2^2}{2k_1 \kappa_2} \sin k_1 L_W \sinh \kappa_2 L_B, \end{aligned} \quad (1)$$

where  $k_1$  and  $\kappa_2$  are the wave vectors in the wells, and in the barrier, respectively. The subscripts  $W$  and  $B$  in Eqs. (1) denote the wells or barriers, and  $L = L_W + L_B$  is the SL period. The wave vectors in the well and barrier are

$$\begin{aligned} k_1 &= \sqrt{\frac{2m_W E}{\hbar^2}} \\ \kappa_2 &= \sqrt{\frac{2m_B (V - E)}{\hbar^2}}. \end{aligned} \quad (2)$$

The above equations can be solved for electrons and holes separately, obtaining the relation  $E(K)$  where  $E$  is the electron/hole energy,  $m_W$  and  $m_B$  are effective masses in Cu<sub>2</sub>O and MgO, and  $V$  is the potential barrier between MgO and Cu<sub>2</sub>O. Specifically, due to the difference of band gap energies (see Table I), we have  $V_0 = 4.99$  eV. From this, we obtain the electron and hole confinement

potentials  $V_{0e,h}$

$$\begin{aligned} V_0 &= E_g(\text{MgO}) - E_g(\text{Cu}_2\text{O}), \\ V_0 &= V_{0e} + V_{0h}, \\ V_{0e} &= 0.4 \times V_0, \quad V_{0h} = 0.6 \times V_0. \end{aligned} \quad (3)$$

This results in two barrier values  $V_{0e} = 2$  eV and  $V_{0h} = 3$  eV for electrons and holes, respectively. The division of  $V_0$  into electron and hole potential barriers follows from the relative Fermi energy level of  $\text{Cu}_2\text{O}$ <sup>29</sup> and  $\text{MgO}$ <sup>30</sup> and is similar to the case of  $\text{Cu}_2\text{O}/\text{ZnO}$  heterojunction<sup>31</sup>.

One of the important parameters of SL structure that differentiates it from bulk material are the effective masses of a hole and an electron in the  $z$  direction, which are determined from the relation

$$\frac{1}{m_z} = \frac{1}{\hbar^2} \frac{d^2 E}{dK^2} \Big|_{K=0}. \quad (4)$$

which, again, can be obtained separately for electrons and holes, from the respective  $E(k)$  relations.

### III. OPTICAL PROPERTIES

We consider a superlattice consisting of multiple layers of wells and barriers, characterized by a thickness  $L_W$  and  $L_B$  and a total thickness of a single well-barrier pair  $L$ . The system is presented in Fig. 1. It is irradiated by a normally incident electromagnetic wave, linearly polarized in the  $x$ -direction

$$E_i(z, t) = E_{i0} \exp(ik_0 z - i\omega t), \quad k_0 = \frac{\omega}{c}. \quad (5)$$

We assume that  $L < 4$  nm. The total number of layers is on the order of 10-100, and the exact number is not relevant to the calculations.

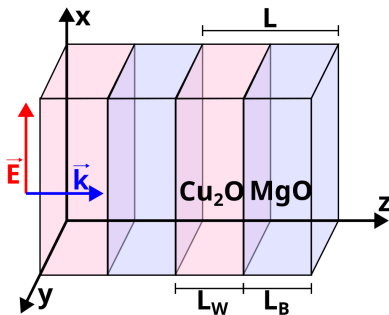


FIG. 1: Schematic representation of the system.

The linear optical response of the system (here we consider the lowest electron and hole miniband) to the electromagnetic wave originates from a given pair of minibands, and is described by two equations: the so-called constitutive equation (material equation) and the Maxwell's propagation equation. The constitutive equation has the form

$$-i\hbar\partial_t Y - i\Gamma Y + H_{eh} Y = \mathbf{M}(\mathbf{r})\mathbf{E}(\mathbf{R}), \quad (6)$$

where  $Y(\mathbf{R}, \mathbf{r}, t)$  is the excitonic transition coherent amplitude,  $\Gamma$  is a dissipation coefficient,  $\mathbf{M}$  is the transition dipole density,  $\mathbf{R}$  is the excitonic center-of-mass coordinate, and  $\mathbf{r}$  the relative electron hole-coordinate. The operator  $H_{eh}$  is the effective mass Hamiltonian of the superlattice

$$H_{eh} = E_g + \frac{P_Z^2}{2M_z} + \frac{\mathbf{P}_{\parallel}^2}{2M_{\parallel}} + \frac{p_z^2}{2\mu_z} + \frac{\mathbf{p}_{\parallel}^2}{2\mu_{\parallel}} + V_{eh}, \quad (7)$$

with  $V_{eh}$  being the electron-hole Coulomb interaction. We have separated the center-of-mass coordinate  $\mathbf{R}_{\parallel}$  and the related momentum  $\mathbf{P}_{\parallel}$  from the relative coordinate  $\rho$  on the plane  $x-y$  and the related momentum  $\mathbf{p}_{\parallel}$ . In the above formulas the reduced mass in the  $z$ -direction is given by

$$\frac{1}{\mu_z} = \frac{1}{m_{ez}} + \frac{1}{m_{hz}}, \quad (8)$$

where the electron- and the hole effective masses in the  $z$ -direction follow from the miniband dispersion relations (1), one for electrons and one for holes, respectively. The system is not confined in  $xy$  directions and so the in-plane effective masses  $m_{\parallel}$  in the well material are assumed to be the same as in bulk medium.  $M_z$  and  $M_{\parallel}$  are the total excitonic masses in the growth direction and parallel to the layers, respectively. We use the same form for the transition dipole density, as for bulk semiconductor<sup>26</sup>

$$\begin{aligned} \mathbf{M}(\mathbf{r}) &= \mathbf{e}_r M_{10} \frac{r+r_0}{2r^2 r_0^2} e^{-r/r_0} = \mathbf{e}_r M(r) \\ &= \mathbf{i} M_{10} \frac{r+r_0}{4ir^2 r_0^2} \sqrt{\frac{8\pi}{3}} (Y_{1,-1} - Y_{1,1}) e^{-r/r_0} \\ &\quad + \mathbf{j} M_{10} \frac{r+r_0}{4r^2 r_0^2} \sqrt{\frac{8\pi}{3}} (Y_{1,-1} + Y_{1,1}) e^{-r/r_0} \\ &\quad + \mathbf{k} M_{10} \frac{r+r_0}{2r^2 r_0^2} \sqrt{\frac{4\pi}{3}} Y_{10} e^{-r/r_0}, \end{aligned} \quad (9)$$

where  $r_0$  is the so-called coherence radius

$$r_0^{-1} = \sqrt{\frac{2\mu}{\hbar^2} E_g}. \quad (10)$$

The above expression gives the coherence radius in terms of effective band parameters  $E_g$  (the bulk gap energy), and  $\mu$  (the electron-hole reduced effective mass, the bulk effective masses of the electron and the hole are assumed to be isotropic).  $M_{10}$  is the integrated dipole strength. In order to present detailed derivation of susceptibility with Rydberg excitons adapted for a case of a superlattice we recall the procedure similar to that presented in<sup>26</sup>. The steps of the calculation scheme are the following:

1. The excitonic amplitude  $Y$  is determined from Eq. (6) with the Hamiltonian (7).

2. The coherent amplitude  $Y$  enables to calculate the SL polarization which is given by the formula<sup>26</sup>

$$\mathbf{P}(\mathbf{R}) = 2 \int d^3r \mathbf{M}(\mathbf{r}) Y(\mathbf{R}, r). \quad (11)$$

3. The polarization  $\mathbf{P}$  is then inserted into the Maxwell propagation equation

$$c^2 \nabla_R^2 \mathbf{E} - \underline{\epsilon}_b \ddot{\mathbf{E}}(\mathbf{R}) = \frac{1}{\epsilon_0} \ddot{\mathbf{P}}(\mathbf{R}), \quad (12)$$

with the use of the bulk dielectric tensor  $\underline{\epsilon}_b$  and the vacuum dielectric constant  $\epsilon_0$ .

In analogy to bulk crystals, the description of SL exciton-polaritons is based on the separation of the relative electron-hole motion with well-defined quantum levels and the center-of-mass motion which interacts with the radiation field and produces the mixed modes (polaritons). We assume that the center-of-mass motion is described by the term  $\exp(i\mathbf{k}\mathbf{R})$  with the wave vector  $\mathbf{k}$ . Additionally, we use the EM wave that has a harmonic time dependence  $\propto \exp(-i\omega t)$ . These simplifications allow us to calculate the dielectric susceptibility. Because in  $\text{Cu}_2\text{O}$  the conduction band and the valence band are of the same parity the dipole moment between them vanishes; the  $n > 1$  lines correspond to excitons with the relative angular momentum  $l = 1$  therefore the absorption process is dipole-allowed. The Eq. (6) will be solved by expanding the coherent amplitude  $Y$  in terms of eigenfunctions of the Hamiltonian  $H_{eh}$ ,

$$Y = \sum_{n\ell m} c_{n\ell m} R_{n\ell m}(r) Y_{\ell m}(\theta, \phi), \quad (13)$$

where  $n, l, m$  are main, relative momentum and magnetic quantum numbers respectively,  $Y_{\ell m}$  are spherical harmonics, which are real valued functions of the spherical coordinates  $\theta, \phi$ . Specifically, we use the definition

$$Y_{\ell, m}(\theta, \phi) = \sqrt{\frac{2\ell + 1}{4\pi} \frac{(\ell - m)!}{(\ell + m)!}} P_{\ell}^m(\cos \theta) e^{im\phi}, \quad (14)$$

where  $P_{\ell, m}$  are the associated Legendre polynomials,

$$P_{\ell}^m(x) = \frac{(-1)^m}{2^{\ell} \ell!} (1 - x^2)^{m/2} \frac{d^{\ell+m}}{dx^{\ell+m}} (1x^2)^{\ell}. \quad (15)$$

The radial functions  $R_{n\ell m}$  are given in the form

$$R_{n\ell m}(r) = \left( \frac{2\eta_{\ell m}}{na^*} \right)^{3/2} \frac{1}{(2\ell + 1)!} \sqrt{\frac{(n + \ell)!}{2n(n - \ell - 1)!}} \times \left( \frac{2\eta_{\ell m} r}{na^*} \right)^{\ell} e^{-\eta_{\ell m} r / na^*} M \left( -n + \ell + 1, 2\ell + 2, \frac{2\eta_{\ell m} r}{na^*} \right). \quad (16)$$

The coefficient  $\eta_{\ell m}$  depends on an effective masses ratio  $\alpha$ , which for SL is different from the bulk and therefore is crucial for eigenvalues  $E_{n\ell m}$

$$\eta_{\ell m} = \int d\Omega \frac{|Y_{\ell m}|^2}{\sqrt{\sin^2 \theta + \alpha \cos^2 \theta}}, \quad (17)$$

$$E_{n\ell m} = -\frac{\eta_{\ell m}^2(\alpha) R^*}{n^2}, \quad n = 1, 2, \dots, \\ \ell = 0, 1, 2, \dots, n - 1, \quad m = 0, 1, 2, \dots, \ell, \\ \alpha = \frac{\mu_{\parallel}}{\mu_z}. \quad (18)$$

$a^*$  is the exciton Bohr radius,  $M(a, b, z)$  is the Kummer function (confluent hypergeometric function) in the notation of Ref.<sup>32</sup>. The anisotropy parameter  $\alpha$ , first introduced by Kohn and Luttinger<sup>33</sup>, corresponds to the dimensionality of the system<sup>34,35</sup>; specifically in the so-called Fractional Dimensionality Approach<sup>36</sup>, the system dimension  $d = 2 + \sqrt{\alpha}$ , so that it is two-dimensional in the limit of  $\alpha \rightarrow 0$  and 3-dimensional for  $\alpha = 1$ .

$R^*$  is the effective excitonic Rydberg energy defined as

$$R^* = \frac{\mu_{\parallel} e^4}{2(4\pi\epsilon_0\sqrt{\epsilon_{\parallel}\epsilon_z})^2 \hbar^2}. \quad (19)$$

With the modified by periodic potential of SL effective masses, one can calculate the anisotropy factor  $\alpha$  and the corresponding eigenvalues  $E_{n\ell m}$  from eq.(18). In the considered case of  $P$  excitons we use the quantities

$$\eta_{00}(\alpha) = \frac{\arcsin \sqrt{1 - \alpha}}{\sqrt{1 - \alpha}}, \\ \eta_{10}(\alpha) = \frac{3}{2(1 - \alpha)} (\eta_{00} - \sqrt{\alpha}), \\ \eta_{11}(\alpha) = \frac{3}{2} \left[ \eta_{00}(\alpha) - \frac{1}{3} \eta_{10}(\alpha) \right]. \quad (20)$$

The energies for electron and hole  $E_{0e,h} = E_{e,h}(k = 0)$  determine the SL energy gap

$$E_g(\text{SL}) = E_g + E_{0e} + E_{0h}, \quad (21)$$

which is shifted and, together with the eigenenergies  $E_{n\ell m}$ , the positions of SL excitonic resonances, given by the transverse energies  $E_{Tn\ell m}$

$$E_{Tn\ell m} = E_g(\text{SL}) + E_{n\ell m}, \quad (22)$$

which are also moved due to the modification of effective masses by the influence of SL periodic potentials pattern.

Since the superlattice consists of multiple quantum wells, it is justified to assume that symmetry properties of excitons in SL are similar to these in quantum wells. The considered system geometry (see Fig. 1) and the electric field polarization (5) allows to use the  $\mathbf{i}$ -component of the dipole density (9),

$$M_x(r) = M_{10} \frac{r + r_0}{4r^2 r_0^2} \sqrt{\frac{8\pi}{3}} (Y_{1,-1} - Y_{1,1}) e^{-r/r_0}. \quad (23)$$

With the help of Eqs. (16) and (23) the expansion coefficients  $c_{n\ell m}$  are calculated. Then the coherent amplitude  $Y$  is used in Eq. (11), which in turn is inserted into

the Maxwell equation (12), from which one obtains the dispersion relation for SL-polaritons

$$\frac{c^2 k^2}{\omega^2} - \epsilon_b \quad (24)$$

$$= \epsilon_b \sum_{n=2}^N \frac{\Delta_{LT}^{(P)} f_{n11}}{E_{Tn11} - \hbar\omega + (\hbar^2 k^2 / 2M_z) - i\Gamma_n},$$

with

$$f_{n11} = \frac{32}{3} \frac{(n^2 - 1)\eta_{11}^5}{n^5}. \quad (25)$$

$\Delta_{LT}^{(P)}$  is the longitudinal-transversal splitting energy, and  $E_{Tn11}$  are the energies of excitonic resonances (see Eq. (22)). The relation<sup>37</sup>

$$|M_{10}|^2 = \frac{4\epsilon_0\epsilon_b a^{*3} \Delta_{LT}^{(P)}}{\pi(r_0/a^*)^2},$$

has been used. In the considered, narrow frequency range, one can use  $\epsilon_b = const = 7.5^{11}$ .

The spatial dispersion, described by (24), makes it possible to have two or more wave modes connected with a given frequency. The term  $\hbar^2 k^2 / 2M_z$  in the denominator on r.h.s. of Eq. (24) is responsible for the effect of multiplicity of polariton waves. In the considered case of Cu<sub>2</sub>O/MgO SL the total exciton mass  $M_z$  is much larger than in other semiconductors (both bulk and SL) so it is justified to neglect this term. As pointed out in<sup>38</sup>, relatively small oscillator strength and resulting weak light-exciton coupling in bulk Cu<sub>2</sub>O makes it difficult to achieve strong coupling regime necessary for polaritonic effects to become significant. It is demonstrated in<sup>38</sup> that this problem can be solved by placing the crystal between two Bragg reflectors, forming a cavity; multiple, strong reflections on Cu<sub>2</sub>O/MgO interfaces considered here might provide another way of achieving strong coupling regime. In view of the above findings, we obtain the excitonic contribution to the linear optical susceptibility in the form  $\chi(\omega)$ ,

$$\chi(\omega) = \epsilon_b \sum_{n=2}^N \frac{\Delta_{LT}^{(P)} f_{n11}}{E_{Tn11} - \hbar\omega - i\Gamma_n}. \quad (26)$$

In particular, we are interested in the imaginary part of susceptibility, where absorption maxima corresponding to excitonic states can be observed; we note that apart from these maxima, both Cu<sub>2</sub>O and MgO are mostly transparent, with significant absorption occurring only on a length scale of tens of  $\mu\text{m}$ .

#### IV. RESULTS

The above presented scheme allows the calculation of all optical SL functions. We have chosen the optical susceptibility since its imaginary part is proportional to

the SL absorption. We have computed the susceptibility Cu<sub>2</sub>O/MgO SL for a variety of Cu<sub>2</sub>O QW and MgO barrier thicknesses. The values of the relevant parameters are given in Table I. The obtained results are illustrated in Figures 2-9.

The Fig. 2 presents the imaginary part of susceptibility of bulk Cu<sub>2</sub>O and a superlattice with  $L=4$  nm ( $L_W = L_B = 2$  nm). Even for such a relatively large  $L$  (on the order of 10 lattice constants), the energy shifts  $E_{e0}$ ,  $E_{h0}$  are considerably larger than energy spacing of excitonic levels. The two key features visible in Fig. 2 is a

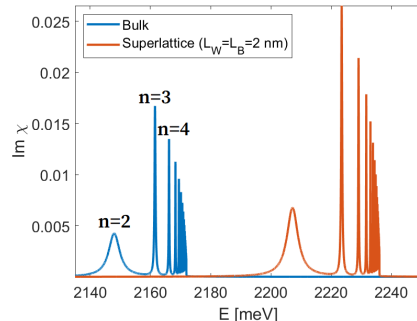


FIG. 2: Comparison of the imaginary part of susceptibility in bulk Cu<sub>2</sub>O and in Cu<sub>2</sub>O/MgO SL, calculated from Eq. (26). First few excitonic states  $n = 2..4$  are marked.

slight increase of oscillator strength (proportional to the area under the absorption peak) is SL, as well as a slight modification of Rydberg energy, in accordance with Eq. (19).

As the SL period  $L$  is decreased, the energy shift increases proportionally to  $\sim 1/L$ . This is shown in Fig. 3 a). For values  $L < 4$  nm, the shift exceeds the total width of excitonic spectrum which means that the confinement energy exceeds the Rydberg energy. It should be stressed that the energy shift of excitonic spectrum is very considerable, exceeding 1 eV for  $L < 1$  nm. By omitting the energy shifts  $E_{e0}$ ,  $E_{h0}$  (Fig. 3 b), one can see the smaller effects; As  $L$  decreases, there is a slight decrease of Rydberg energy; one can see this by comparing spectra in Fig. 3 b) with dashed, vertical lines that mark  $n=2$  exciton energy and gap energy for  $L = 6$  nm, which is close to bulk. For small values of  $L$ , the excitonic spectrum becomes visibly narrower, which is a result of smaller effective Rydberg energy  $\eta_{lm}^2(\alpha)R^*$ .

As a next step, one can calculate the dispersion relation from Eq. (24). The results for 3 values of  $L$  ( $L_W = L_B = L/2$ ) are shown in Fig. 4. For clarity, an energy region near  $n=2$  exciton is chosen; similar shape of the function  $E(k)$  is present for every excitonic resonance ( $n=3$  is visible in upper right corner). Overall, the excitons result in a small, localized disturbance of the bulk dispersion relation (dashed line) which is energy shifted depending on the value of  $L$ .

To calculate the relevant quantities, such as electron

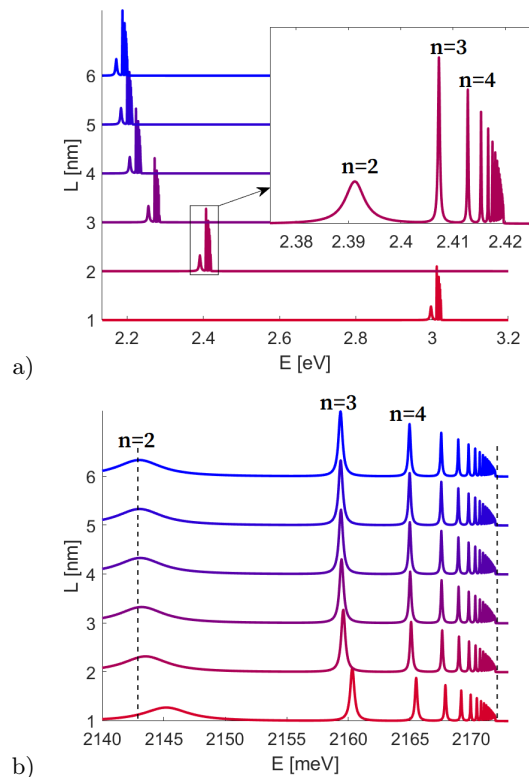


FIG. 3: Imaginary part of superlattice susceptibility a) with and b) without lowest Cu<sub>2</sub>O/MgO SL band energy shift included. Inset: zoom on excitonic spectrum for  $L=2$  nm.

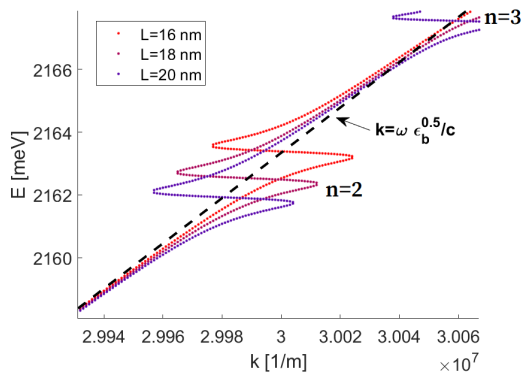


FIG. 4: Polariton dispersion relation of Cu<sub>2</sub>O/MgO superlattice, calculated from Eq.(24), for three values of SL period  $L$ , in the energy region of  $n=2$  exciton.

Dashed line marks dispersion relation calculated for  $\epsilon_b = 7.5$ , without excitonic effects.

and hole effective masses in the  $z$  direction and the anisotropy parameter  $\alpha$ , one has to solve numerically the Eq. (1). The results obtained for a few selected values of  $L_W$ ,  $L_B$  are presented in Fig. 5. For the smallest well and barrier widths, approximately equal to a sin-

gle atomic layer, only two electron/hole band pairs are visible in the energy range  $E < 5$  eV. The lowest band is characterized by a positive effective mass, while the masses in the second band are negative and relatively small ( $\partial^2 E / \partial k^2 \ll 0$ ). The increase of well thickness and barrier thickness both result in a higher density of bands, although the effect of increased  $L_B$  is less significant. Notably, the dispersion relation of the lowest band becomes extremely flat, especially for holes ( $\partial^2 E / \partial k^2 \rightarrow 0$ ), which results in a very big hole effective mass in the  $z$  direction.

The Fig. 6 depicts the effective electron and hole masses (Eq. (4) as well as anisotropy parameter  $\alpha$  (Eqs. (8) and (18)) as a function of  $L_W$ , where  $L_W + L_B = 1.4$  nm. One can see that there is some optimal value of  $L_W = 0.5$  nm,  $L_B = 1.5$  nm, where effective masses are maximized the anisotropy parameter reaches minimum value  $\alpha \approx 0.25$  for a slightly smaller well width. As mentioned above, the effective mass of the hole can reach a very high value in the considered system, up to  $m_z \sim 70 m_0$ , while the effective electron mass does not exceed  $3 m_0$ . Significantly increased effective mass in  $z$  direction means that the system approaches a quasi two-dimensional one, with only two degrees of freedom ( $x, y$ ) for exciton motion. This is reflected in a small value of anisotropy parameter  $\alpha$ .

An overview of effective mass values for a range of  $L_W$ ,  $L_B$  is shown in Fig. 7. In the limit of wide barriers, the effective mass of a hole can reach values of up to  $10^3 m_0$ . In practice, this means that the hole cannot tunnel through the potential barrier and the system becomes two dimensional, allowing only for the motion in  $xy$  plane; in such a case, the structure is no longer a superlattice, but a set of separated quantum wells (a multi-well system). The obtained results confirm that the barrier width should not considerably exceed the Bohr radius of the exciton (1.1 nm). It should be stressed that the small barrier width is a necessary condition for the tunnelling to occur, which is needed for validity of the presented approach. Another effect visible in Fig. 7 is that in the case of a narrow well ( $L_W < 1$  nm), the increase of effective mass is slower due to the fact that the well thickness is smaller than exciton diameter, so that its wavefunction enters the barriers, facilitating easier tunneling through them.

Fig. 8 depicts the lowest polariton band energy as a function of  $L_W$ ,  $L_B$ . One can see that the energy dependence on well width is much more pronounced, resulting in  $E_{0e} \sim 0.8$  eV and  $E_{0h} \sim 2.2$  eV for  $L_W = 0.4$  nm. This result is analogous to the case of quantum well, where the energy of the lowest level strongly depends on the well width.

Finally, in Fig 9 one can see that the effective oscillator strength of the excitons is slightly enhanced in SL, in particular when both barrier and well thickness is large. This is expected result - as the effective masses  $m_{ez}$ ,  $m_{hz}$  and increase, the reduced mass  $\mu_z$  (Eq. (8)) also increases and anisotropy parameter  $\alpha$  (Eq. (18)) is decreasing. This, according to Eq. (20), affects the oscilla-

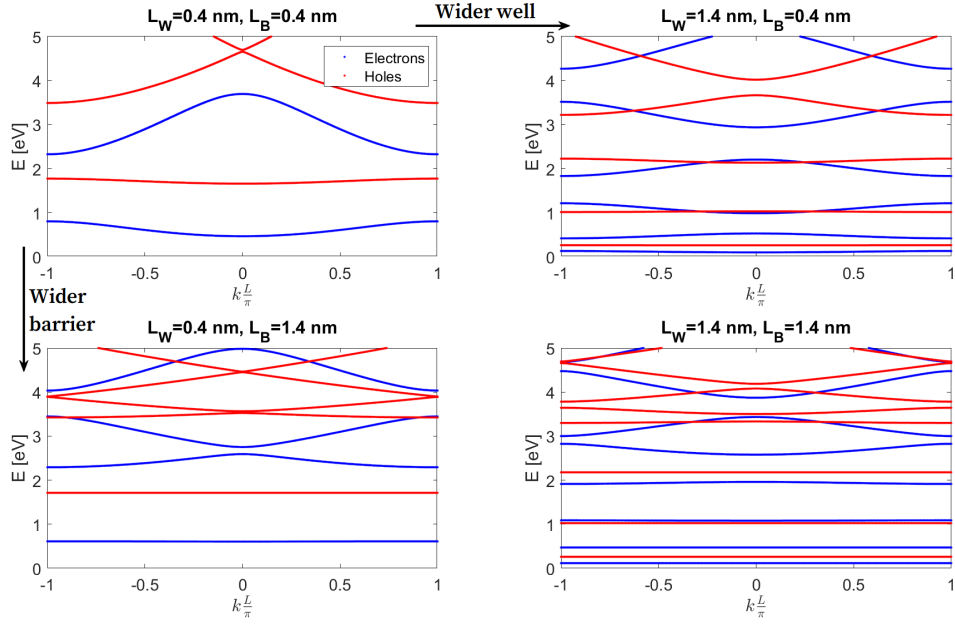


FIG. 5: SL Dispersion relations of electrons and holes, calculated from Eq. (1) for various values of well ( $L_W$ ) and barrier ( $L_B$ ) widths.

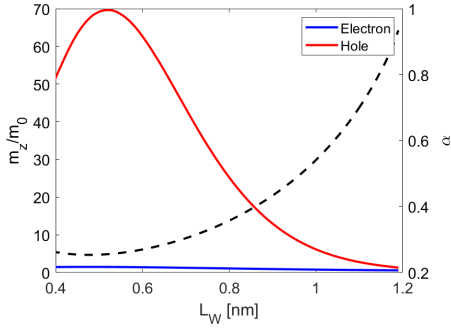


FIG. 6: Electron and hole effective masses (Eq. (4), left axis) and anisotropy parameter  $\alpha$  (calculated from Eqs. (8) and (18), right axis) of  $\text{Cu}_2\text{O}/\text{MgO}$  SL, as a function of  $L_W$ ;  $L_W + L_B = 1.4$  nm.

tor strength.

Superlattice containing  $\text{Cu}_2\text{O}$  can use various barrier materials; one of the possibilities is  $\text{ZnO}$ <sup>31</sup>. In contrast to  $\text{MgO}$ ,  $\text{ZnO}$  is a semiconductor with relatively narrow band gap  $E_g = 3.4$  eV<sup>39</sup>, which results in barrier energies of  $E_{0e} = 0.7$  eV and  $E_{0h} = 1.88$  eV. The relatively small value of the barrier yields low effective masses in  $z$  direction and a large value of  $\alpha$ . Results of calculations are shown in Fig. 10. The material parameters used in calculations are given in Table. I.

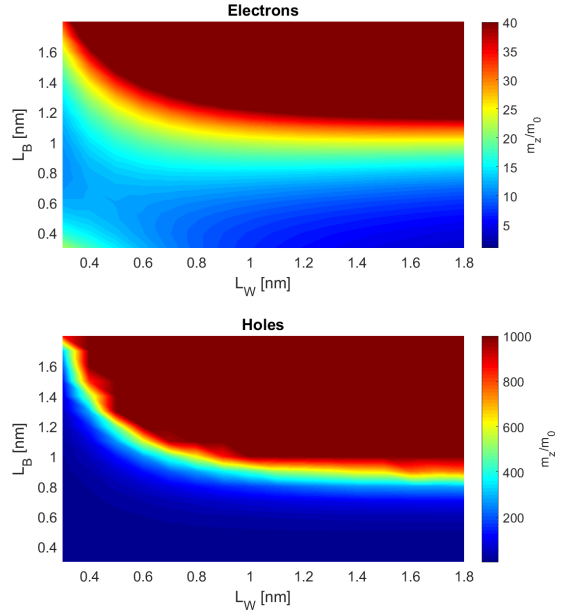


FIG. 7: Electron and hole effective masses in  $\text{Cu}_2\text{O}/\text{MgO}$  SL as a function of  $L_W$  and  $L_B$ , calculated from Eq. (4).

## V. CONCLUSIONS

In conclusion, we have developed a simple mathematical procedure to calculate in analytical form the susceptibility of superlattice with Rydberg excitons taking as

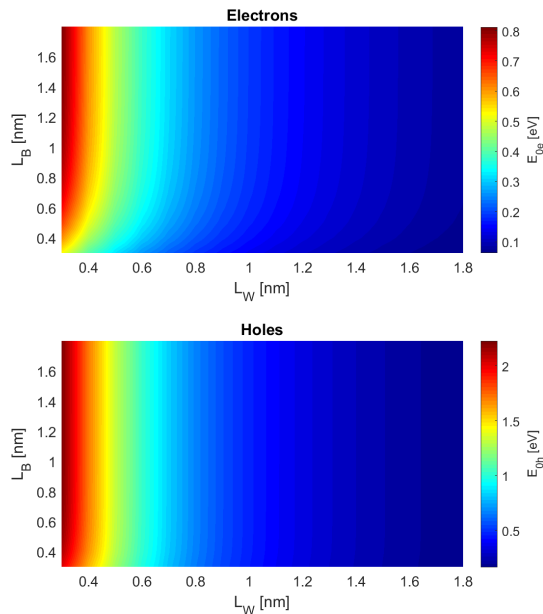


FIG. 8: The energy of the lowest electron and hole band in  $\text{Cu}_2\text{O}/\text{MgO}$  SL, as a function of  $L_W$  and  $L_B$ , calculated from Eq. (1).

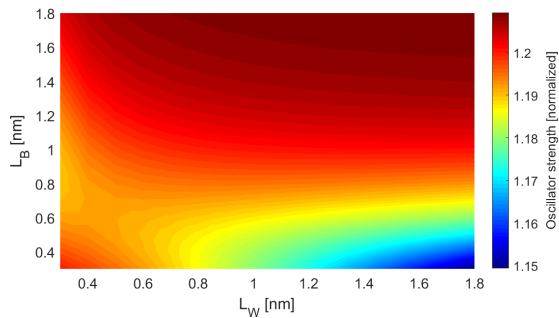


FIG. 9: Exciton oscillator strength in  $\text{Cu}_2\text{O}/\text{MgO}$  SL, as a function of  $L_W$  and  $L_B$ , calculated from Eq. (25), normalized to the bulk value.

an example  $\text{Cu}_2\text{O}/\text{MgO}$  SL, in the case of normal incidence of the exciting electromagnetic wave. With the help of Kronig-Penney model for superlattice we have calculated effective masses of a hole and electron and then used real density matrix approach to obtain resonances for any REs and the polariton dispersion relation. Periodic potentials of the SL structure causes the change of effective masses, which results in the increase of oscillator strengths and significantly shifts positions of the excitonic resonances by over 1 eV. This sensitivity of the energy of excitonic resonances to the SL dimensions may provide an efficient way of measuring mechanical deformation and temperature via thermal expansion of the lattice. The influence of the SL geometry, i.e., the well and barrier thicknesses, on an excitonic spectrum and the dis-

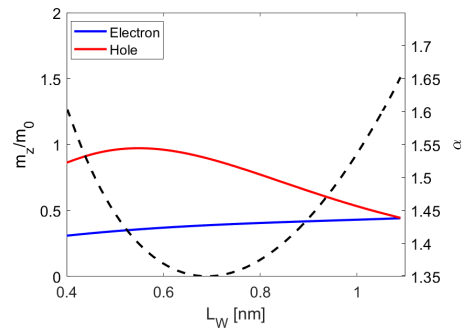


FIG. 10: Electron and hole effective masses (Eq. (4), left axis) and anisotropy parameter  $\alpha$  (calculated from Eqs. (8) and (18), right axis) of  $\text{Cu}_2\text{O}/\text{ZnO}$  SL, as a function of  $L_W$ ;  $L_W + L_B = 1.4$  nm.

TABLE I: Parameter values for bulk  $\text{Cu}_2\text{O}$ ,  $\text{MgO}$  and  $\text{ZnO}$ ; masses in free electron mass  $m_0$ ,  $R^*$  calculated from  $(\mu/\epsilon_b^2) \cdot 13600$  meV,  $R_{e,h}^* = (m_{e,h}/\mu)R^*$ , <sup>(a)</sup> calculated by the assumption that the masses in the  $x-y$  plane remain unaltered, lengths in nm,  $a_{e,h}^* = (\mu/m_{e,h})a^*$

Parameter	$\text{Cu}_2\text{O}$ (Bulk)	$\text{MgO}$ (Bulk)	$\text{ZnO}$ (Bulk)	References
$E_g$	2172.08	7160	3400	11,39,40
$R^*$	87.78		60	39
$\Delta_{LT}$	0.0125			14
$m_{ez}$	0.99	0.378	0.24	39,41-43
$m_{h\parallel}$	0.58	1.575	0.54	39,41-43
$m_{hz}$	0.58	1.575	0.54	39,41-43
$\mu_{\parallel}$	0.363	0.319	0.17	
$\mu_z$	0.363	0.319	0.17	
$M_z$	1.56	1.953	0.83	
$\alpha$	1	1	1	
$a^*$	1.1			11
$r_0$	0.22			26
$\epsilon_b$	7.5		8.656	11,39
$\Gamma_j$	$3.88/j^3$			11,13

person relation have been examined. It turned out that the periodic potential of the considered geometry leads to a significant anisotropy and either small or large value of the anisotropy factor  $\alpha$ , which can be tuned depending on intended structure application. Finally, we note that Rydberg excitons confined in a superlattice may be a promising platform for quantum computing technologies, being a solid-state analogue of an atomic optical lattice, with significant advantage of compactness and higher operating temperatures.



## VI. ACKNOWLEDGMENTS

Support from the National Science Centre, Poland (NCN), project Miniatura, 2022/06/X/ST3/01162, is greatly acknowledged.

- 
- \* david.ziemkiewicz@utp.edu.pl
- <sup>1</sup> C. Klingshirn, *Semiconductor optics*, 2nd Ed. (Springer, Berlin-Heidelberg 2005, ISBN 3-540-21328-7)
  - <sup>2</sup> D. Harankahage, J. Cassidy, M. Yang, D. Porotnikov, M. Williams, N. Kholmicheva, and M. Zamkov, Quantum Computing with Exciton Qubits in Colloidal Semiconductor Nanocrystals, *The Journal of Physical Chemistry C* **125**, 40, 22195 (2021).
  - <sup>3</sup> Y. Zhang, X. Zhang, B. Tang, C. Tian, C. Xu, H. Dong, and W. Zhou, Realization of an all-optically controlled dynamic superlattice for exciton-polaritons, *Nanoscale* **10**, 14082 (2018).
  - <sup>4</sup> S. Ghosh, Timothy C. H. Liew, Quantum computing with exciton-polariton condensates, *npj Quantum Information* **6**, 16 (2020).
  - <sup>5</sup> X. Zang, S. Montangero, L. D. Carr, and M. T. Lusk, Engineering and manipulating exciton wave packets, *Phys. Rev. B* **95**, 195423 (2017).
  - <sup>6</sup> M.J. Yang, P.V. Wadekar, W.C. Hsieh, H.C. Huang, C.W. Lin, J.W. Chou, C.H. Liao, C.F. Chang, H.W. Seo, S.T. You, L.W. Tu, I.K. Lo, N.J. Ho, S.W. Yeh, H.H. Liao, Q.Y. Chen, and W.K. CHu, MgO/Cu<sub>2</sub>O superlattices: Growth of Epitaxial, Two-Dimensional Nanostructures, *J. of Electronic Materials* **45**, 62856291 (2016).
  - <sup>7</sup> L. Isenhower, E. Urban, X. L. Zhang, A. T. Gill, T. Henage, T. A. Johnson, T. G. Walker, and M. Saffman, Demonstration of a Neutral Atom Controlled-NOT Quantum Gate, *Phys. Rev. Lett.* **104**, 010503 (2010).
  - <sup>8</sup> A. Omran, H. Levine, A. Keesling, G. Semeghini, T. T. Wang, S. Ebadi, H. Bernien, A. S. Zibrov, H. Pichler, S. Choi, J. Cui, M. Rossignolo, P. Rembold, S. Montangero, T. Calarco, M. Endres, M. Greiner, V. Vuletic and M. D. Lukin, Generation and manipulation of Schrödinger cat states in Rydberg atom arrays, *Science* **365** (6453), 570 (2019).
  - <sup>9</sup> W. Li, A boost to Rydberg quantum computing, *Nature Physics* **16**, 820 (2020).
  - <sup>10</sup> A.V. Mazanik, A.I. Kulak, E.A. Bondarenko, O.V. Korolik, N.S. Mahon, E.A. Streltso, Strong room temperature exciton photoluminescence in electrochemically deposited Cu<sub>2</sub>O films, *Journal of Luminescence* **251**, 119227 (2022).
  - <sup>11</sup> T. Kazimierzuk, D. Fröhlich, S. Scheel, H. Stolz, and M. Bayer, Giant Rydberg excitons in the copper oxide Cu<sub>2</sub>O, *Nature* **514**, 344 (2014).
  - <sup>12</sup> M. A. M. Versteegh, S. Steinhauer, J. Bajo, T. Lettner, A. Soro, A. Romanova, S. Gyger, L. Schweickert, A. Mysyrowicz and V. Zwiller, Giant Rydberg excitons in Cu<sub>2</sub>O probed by photoluminescence excitation spectroscopy, *Phys. Rev. B* **104**, 245206 (2021).
  - <sup>13</sup> D. Ziemkiewicz, S. Zielińska-Raczyńska, *Optics Express* **27** Solid-state pulsed microwave emitter based on Rydberg excitons, 16983, (2019).
  - <sup>14</sup> H. Stolz, F. Schöne, and D. Semkat, Interaction of Rydberg Excitons in Cuprous Oxide with Phonons and Photons: Optical Linewidth and Polariton Effect, *New. J. Phys.* **20**, 023019, (2018).
  - <sup>15</sup> C. Morin, J. Tignon, J. Mangeney, S. Dhillon, G. Czajkowski, K. Karpiński, S. Zielińska-Raczyńska, Da. Ziemkiewicz, and T. Boulier, Self-Kerr Effect across the Yellow Rydberg Series of Excitons in Cu<sub>2</sub>O *Phys. Rev. Lett.* **129**, 137401 (2022).
  - <sup>16</sup> S. Steinhauer, M. Versteegh, S. Gyger, A. Elshaari, B. Kunert, A. Mysyrowicz, and V. Zwiller, Rydberg excitons in Cu<sub>2</sub>O microcrystals grown on a silicon platform, *Commun. Mater.* **1**, 2 (2020).
  - <sup>17</sup> M. Takahata, K. Tanaka, and N. Naka, Nonlocal optical response of weakly confined excitons in Cu<sub>2</sub>O mesoscopic films, *Phys. Rev. B* **97**, 205305 (2018).
  - <sup>18</sup> A. Konzelmann, B. Frank, and H. Giessen, Quantum confined Rydberg excitons in reduced dimensions, *J. Phys. B: At. Mol. Opt. Phys.* **53**, 024001 (2020).
  - <sup>19</sup> D. Ziemkiewicz, G. Czajkowski, K. Karpiński, S. Zielińska-Raczyńska, Nonlinear optical properties and Kerr nonlinearity of Rydberg excitons in Cu<sub>2</sub>O quantum wells, *Phys. Rev. B* **106**, 085431 (2022).
  - <sup>20</sup> D. Ziemkiewicz and S. Zielińska-Raczyńska, Optical-to-microwave frequency conversion with Rydberg excitons, *Phys. Rev. B* **107**, 195303 (2023).
  - <sup>21</sup> K. Orfanakis, S. Rajendran, H. Ohadi, S. Zielińska-Raczyńska, G. Czajkowski, K. Karpiński, and D. Ziemkiewicz, Quantum confined Rydberg excitons in Cu<sub>2</sub>O nanoparticles, *Phys. Rev. B* **103**, 245426 (2021).
  - <sup>22</sup> G. Bastard, *Wave Mechanics Applied to Semiconductor Heterostructures* (Les Editions de Physique, Paris, 1989).
  - <sup>23</sup> M. F. Pereira Jr., I. Galbraith, S. W. Koch, and G. Dugan, *Phys. Rev. B* **42**, 7084 (1990).
  - <sup>24</sup> G. Czajkowski, F. Bassani, and A. Tredicucci, Polaritonic effects in superlattices, *Phys. Rev. B* **54**, 2035 (1996).
  - <sup>25</sup> P. Schillak and G. Czajkowski, Optical properties of anisotropic II-VI superlattices, *Phys. Stat. Sol. B* **244**, 1627 (2007).
  - <sup>26</sup> S. Zielińska-Raczyńska, G. Czajkowski, and D. Ziemkiewicz, Optical properties of Rydberg excitons and polaritons, *Phys. Rev. B* **93**, 075206 (2016).
  - <sup>27</sup> D. Ziemkiewicz, K. Karpiński, G. Czajkowski, and S. Zielińska-Raczyńska, Excitons in Cu<sub>2</sub>O: From quantum dots to bulk crystals and additional boundary conditions for Rydberg exciton-polaritons, *Phys. Rev. B* **101**, 205202 (2020).
  - <sup>28</sup> J. H. Davies, *The physics of low-dimensional semiconductors, An introduction* (Cambridge University Press, Cambridge, 1997).doi.org/10.1017/CBO9780511819070.
  - <sup>29</sup> B. Balamurugan, I. Aruna, and B. R. Mehta, Size-dependent conductivity-type inversion in Cu<sub>2</sub>O nanoparticles, *Phys. Rev. B* **69**, 165419 (2004).
  - <sup>30</sup> M. A. van Huis, A. van Veen, H. Schut, B. J. Kooi, and J. Th. M. De Hosson, Formation of solid Kr nanoclusters in MgO, *Phys. Rev. B* **67**, 235409 (2003).

- <sup>31</sup> S. Siol, J. C. Hellmann, S. D. Tilley, M. Graetzel, J. Morasch, J. Deuermeier, W. Jaegermann, and A. Klein, Band Alignment Engineering at Cu<sub>2</sub>O/ZnO Heterointerfaces, *ACS Appl. Mater. Interfaces* **8**, 33, 21824 (2016).
- <sup>32</sup> M. Abramowitz and I. Stegun, *Handbook of Mathematical Functions* (Dover Publications, New York, 1965).
- <sup>33</sup> J. M. Luttinger and W. Kohn, Motion of Electrons and Holes in Perturbed Periodic Fields, *Phys. Rev.* **97**, 869 (1955).
- <sup>34</sup> H. Mathieu, P. Lefebvre, and Ph. Christol, Simple analytical method for calculating exciton binding energies in semiconductor quantum wells, *Phys. Rev. B* **46**, 4092 (1992).
- <sup>35</sup> Bassani, G. Czajkowski, and A. Tredicucci, Polaritons in anisotropic semiconductors, *Z. Phys. B* **98**, 39 (1995).
- <sup>36</sup> X. He, Fractional dimensionality and fractional derivative spectra of interband optical transitions, *Phys. Rev. B* **42**, 11751 (1990).
- <sup>37</sup> S. Zielińska-Raczyńska, D. Ziemkiewicz, and G. Czajkowski, Magneto-optical properties of Rydberg excitons: Center-of-mass quantization approach, *Phys. Rev. B* **95**, 075204 (2017).
- <sup>38</sup> K. Orfanakis, S. Rajendran, V. Walther, T. Volz, T. Pohl, and H. Ohadi, Rydberg exciton-polaritons in a Cu<sub>2</sub>O microcavity, *Nature Materials* **21**, 767 (2022).
- <sup>39</sup> D.P. Norton, Y.W. Heo, M.P. Ivill, K. Ip, S.J. Pearton, M.F. Chisholm, T. Steiner, ZnO: growth, doping & processing, *Materials Today* **7**, 6, 34 (2004).
- <sup>40</sup> Q. Yan, P. Rinke, M. Winkelkemper, A. Qteish, D. Bimberg, M. Scheffler, C. G. Van de Walle, Strain effects and band parameters in MgO, ZnO, and CdO, *Applied Physics Letters* **101**, 152105 (2012).
- <sup>41</sup> N. Naka, I. Akimoto, M. Shirai, and Ken-ichi Kan'no, Time-resolved cyclotron resonance in cuprous oxide, *Phys. Rev. B* **85**, 035209 (2012).
- <sup>42</sup> C.W. Miller, Zhi-Pan Li, I. K. Schuller, R. W. Dave, J. M. Slaughter, and J. Akerman, Dynamic Spin-Polarized Resonant Tunneling in Magnetic Tunnel Junctions, *Phys. Rev. Lett.* **99**, 047206 (2007).
- <sup>43</sup> J. Wang, Y. Tu, L. Yang, and H. Tolner, Theoretical investigation of the electronic structure and optical properties of zinc-doped magnesium oxide, *Journal of Computational Electronics* **15**, 1521 (2016).